GEOPHYSICAL RESEARCH LETTERS, VOL. 22, NO. 9, PAGES 1077-1080, MAY 1, 1995

Nonsphericity of dust-like tropospheric aerosols: implications for aerosol remote sensing and climate modeling

M. I. Mishchenko, A. A. Lacis, B. E. Carlson, and L. D. Travis

NASA Goddard Institute for Space Studies, New York, New York

Abstract. The nonsphericity of dust-like tropospheric aerosols causes us to question the applicability of using conventional Mie theory to compute their radiative properties. In this paper we compare T-matrix computations of light scattering by polydispersions of randomly oriented nonspherical aerosols and Mie computations for equivalent spheres. We demonstrate that even moderate nonsphericity results in substantial errors in the retrieved aerosol optical thickness if satellite reflectance measurements are analyzed using Mie theory. On the other hand, the use of Mie theory for nonspherical aerosols produces negligible errors in the computation of albedo and flux related quantities, provided that the aerosol size distribution and optical thickness are known beforehand. The first result can be explained by large nonspherical-spherical differences in scattering phase function, while the second result follows from small nonspherical-spherical differences in single-scattering albedo and asymmetry parameter. Our results demonstrate that no cancellation of errors occurs if one consistently uses Mie theory in the retrieval algorithm and then in computing the albedo for the retrieved aerosol optical thickness.

1. Introduction

Evidence that tropospheric aerosols can cause a direct radiative forcing comparable in magnitude, though opposite in sign, to the expected climate forcing by greenhouse gases [*Hansen and Lacis*, 1990; *Penner et al.*, 1994] makes a compelling case for improved efforts to obtain accurate information about the global distribution of tropospheric aerosols and their radiative impact [*Hansen et al.*, 1993]. Planned spacecraft instruments such as MODIS, MISR, EOSP, and POLDER have as a key objective the retrieval of tropospheric aerosol properties, with emphasis on the aerosol optical thickness. As discussed by *Wang and Gordon* [1994], the retrieval of aerosol optical thickness using satellite reflectance measurements requires an aerosol model, namely, the specification of the aerosol scattering phase function and single-scattering albedo. Most often, the scattering properties of aerosols are modeled using conventional Mie theory, which is strictly valid only for the spherical particle shape. Since dust-like tropospheric aerosols are solid and have nonspherical shapes, the applicability of using Mie theory in retrieval algorithms for circumstances in which such aerosols are present is questionable [*Koepke and Hess*, 1988; *von Hoyningen-Huene and Wendisch*, 1994]. In addition to this remote sensing problem of aerosol nonsphericity, there is a second concern regarding the importance of particle shape in GCM-related computations of radiative transfer. In other words, the question is whether or not Mie theory can be used in calculations of the aerosol radiative forcing if the optical thickness and size distribution of aerosols are already known.

Copyright 1995 by the American Geophysical Union.

Paper number 95GL00798
0094-8534/95/95GL-00798$03.00

Carefully addressing the two aspects of the problem of particle nonsphericity requires accurate information regarding scattering properties of aerosols. Unfortunately, laboratory measurements of light scattering by small natural particles are difficult and have been reported in a very few publications [*Perry et al.*, 1978; *Kuik et al.*, 1991]. Importantly, laboratory measurements for scattering angles near 0° and 180° pose special problems, which makes experimental determinations of such key quantities as single-scattering albedo and asymmetry parameter of the phase function typically impractical. Theoretical computations of light scattering by nonspherical aerosols are also very complicated. Since aerosol particles often have sizes comparable to the wavelength of radiation, the Rayleigh approximation for very small particles or the geometrical optics approximation for very large particles are not usually applicable. Also, to be realistic, theoretical computations must address the distribution of natural particles over sizes, shapes, and orientations, in which case traditional techniques such as the discrete dipole approximation [*Flatau*, 1992] become very time-consuming, especially for particle size parameters (the ratio of the particle circumference to the wavelength of the scattered light) exceeding 5.

An efficient rigorous method for computing light scattering by polydisperse, randomly oriented nonspherical particles with sizes comparable to the wavelength has been developed recently [*Mishchenko,* 1991; *Mishchenko and Travis*, 1994a]. The method is based on Waterman's T-matrix approach [*Waterman*, 1971] and provides analytical rather than numerical averaging of scattering characteristics over particle orientations. Because of its high efficiency, the method allows fast computations for realistic nonspherical polydispersions on scientific workstations and thus enables relevant examination of the problem of aerosol nonsphericity. In the following section we study the effect of nonsphericity on the accuracy of aerosol optical thickness retrievals from satellite reflectance measurements. For simplicity, we consider only the case of measurements over the ocean surface because that is the only circumstance for which routine aerosol retrievals are presently performed on an operational basis. In Section 3 we examine the influence of aerosol shape on the albedo of a simple clear-sky model.

2. Effect of particle nonsphericity on the accuracy of aerosol optical thickness retrievals

To make our analysis relevant to current satellite based retrievals, we adopt the basic atmosphere-ocean model used in the AVHRR aerosol retrieval algorithm [*Rao et al.*, 1989]. Specifically, the ocean surface is assumed to be Lambertian with an albedo 0.015, and the atmosphere is assumed to be cloud-free. Also we assume that tropospheric aerosols are confined to the 300-mb layer just above the surface, where they are uniformly mixed with gas (optical thickness of gas 0.017 at 0.63 μm), while the rest of the gaseous atmosphere (gas optical thickness 0.039) is located above the aerosol-gas layer. A particle refractive index of $1.53+0.008i$ is adopted as representative of dust aerosols at 0.63 μm [*cf. d'Almeida et al.*, 1991].

We employ calculations for prolate and oblate spheroids to represent the scattering properties of nonspherical aerosols.

Despite their regular shapes, spheroids adequately reproduce scattering properties of natural ensembles of submicron- and micron-sized, polydisperse nonspherical particles at visible wavelengths as measured by *Perry et al.* [1978]. Furthermore, *Mishchenko and Travis* [1994b] have shown that optical cross sections and phase functions for randomly oriented prolate and oblate spheroids with the same aspect ratio (ratio of the largest to the smallest particle dimensions) are similar despite their quite different shapes. These results suggest that scattering properties of nonspherical particles depend primarily on the overall departure of the particle shape from sphericity as represented by the aspect ratio.

Naturally occurring solid aerosol particles must be expected to be distributed over both shapes and sizes. A study by *Nakajima et al.* [1989] employing morphological analysis of scanning electron microscope images of dust particles from yellow sand events showed a distribution of particle aspect ratios about a mode of ~1.7. Similar measurements by *Okada et al.* [1987] showed aspect ratios ranging from 1 to 2.3 with a mean of 1.4, while *Hill et al.* [1984] found that samples of soil particles could be represented by a mixture of oblate and prolate spheroids with a mode aspect ratio of slightly more than 2. In view of the relatively few reported efforts to quantify natural distributions of aerosol shapes and the apparent uncertainties, we adopt the moderate aspect ratio of 1.7 as an appropriate average. From a previous study [*Mishchenko and Travis*, 1994b], we found that a 'broad' shape distribution of prolate and oblate spheroids with aspect ratios ranging from 1.1 to 2.2 was reasonably well represented by results for spheroids with the aspect ratio set at the single value of 1.7. Therefore, we simply model the aerosol shape distribution by a mixture of prolate and oblate spheroids with this aspect ratio.

As for the size distribution of the particles, *Hansen and Travis* [1974] and *Mishchenko and Travis* [1994b] have demonstrated that in practice most plausible size distributions of spheres and spheroids can be adequately represented by just two parameters, the effective radius $r_{\rm eff}$ and effective variance $v_{\rm eff}$; i.e., different aerosol size distributions that have the same values of the effective radius and effective variance will have essentially identical scattering properties. From the perspective of computational efficiency, the power law distribution has a substantial advantage over the commonly used gamma and log normal distributions with the same $r_{\rm eff}$ and $v_{\rm eff}$ because the latter have a long 'tail' extending to much larger radii than the maximum radius for the equivalent power law distribution. Despite the fact that the T-matrix method is by far the fastest numerical tool for rigorously calculating spheroidal scattering, the computational burden for large particle sizes can be significant. We have therefore adopted the power law distribution given by $n(r) = C$ for $r \le r_1$, $n(r) = C(r_1/r)^3$ for $r_1 \le r \le r_2$, and $n(r) = 0$ for $r > r_2$, where C is a normalization constant, and r is radius if particles are spherical and equal-surface-area-sphere radius if particles are nonspherical. The parameters r_1 and r_2 were chosen such that the effective variance was fixed at 0.2, corresponding to a reasonably wide distribution.

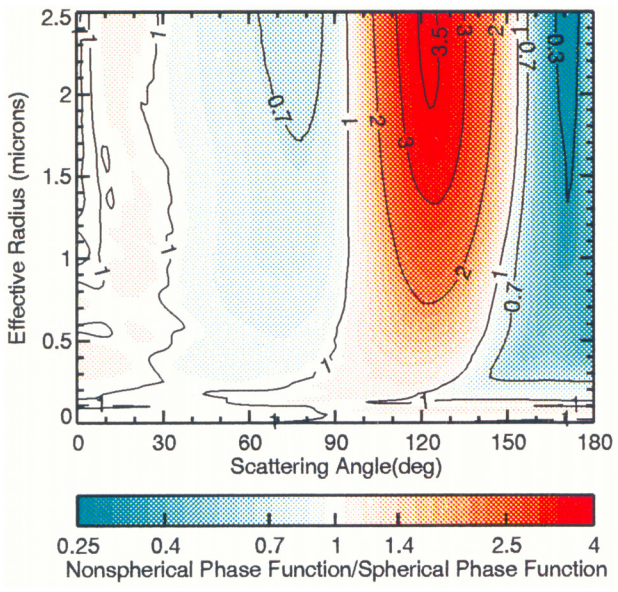

Figure 1. Ratio of nonspherical to spherical phase functions as a function of scattering angle and effective radius. The wavelength is 0.63 μm.

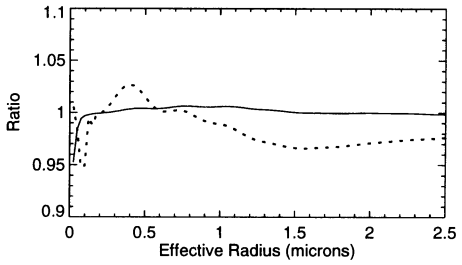

Figure 2. Ratio of nonspherical to spherical single-scattering albedos (solid line) and asymmetry parameters (dotted line) vs effective radius.

Figure 1 shows the ratio of the phase function for polydisperse spheroids relative to that for surface-equivalent spheres as a function of scattering angle and effective radius. Figure 2 shows the corresponding ratios of single-scattering albedos and asymmetry parameters. We see that the phase function ratio can significantly deviate from unity, especially at side-scattering angles around 120°, where it can be as large as 3.55, and at backscattering angles, where it can be as small as 0.248. These computations are in good quantitative agreement with laboratory measurements by *Perry et al.* [1978] for natural nonspherical particles, which suggests that enhanced side-scattering and suppressed backscattering may be universal characteristics of nonspherical phase functions. On the other hand, nonspherical-spherical differences in single-scattering albedo and asymmetry parameter are much less pronounced.

In order to illustrate the level of measurement accuracy that is needed to retrieve aerosol optical thickness from measured reflectivity within some acceptable uncertainty range, let us first assume that aerosols are spherical, and that their size distribution and refractive index are known. Thus, the aerosol optical thickness is the only unknown parameter. We then simulate reflectance measurements by computing the theoretical reflectivity for the atmosphere-ocean model containing aerosols with an effective radius 1 μm and a fixed optical thickness 0.2 and attempt to 'invert' these simulated data using the same spherical particle aerosol model and considering a range of aerosol optical thickness, τ_a, varying from 0 to 1. Figure 3a is a contour plot of the ratio ϱ of the computer-simulated reflectivity for the reference aerosol optical thickness 0.2 relative to the reflectivity computed for the continuously varying optical thickness τ_a. This ratio is plotted as a function of τ_a and cosine of satellite zenith angle μ. The cosine of sun zenith angle is set at 0.9 and the relative satellite-sun azimuth angle at 180° (antisolar azimuth). Multiple-scattering computations have been performed using the standard adding/doubling method and assuming a plane-parallel atmosphere. The $\varrho = 1$ contour corresponds to perfect optical thickness retrieval as a function of μ and is the expected horizontal straight line at the μ-independent value $\tau_a = 0.2$.

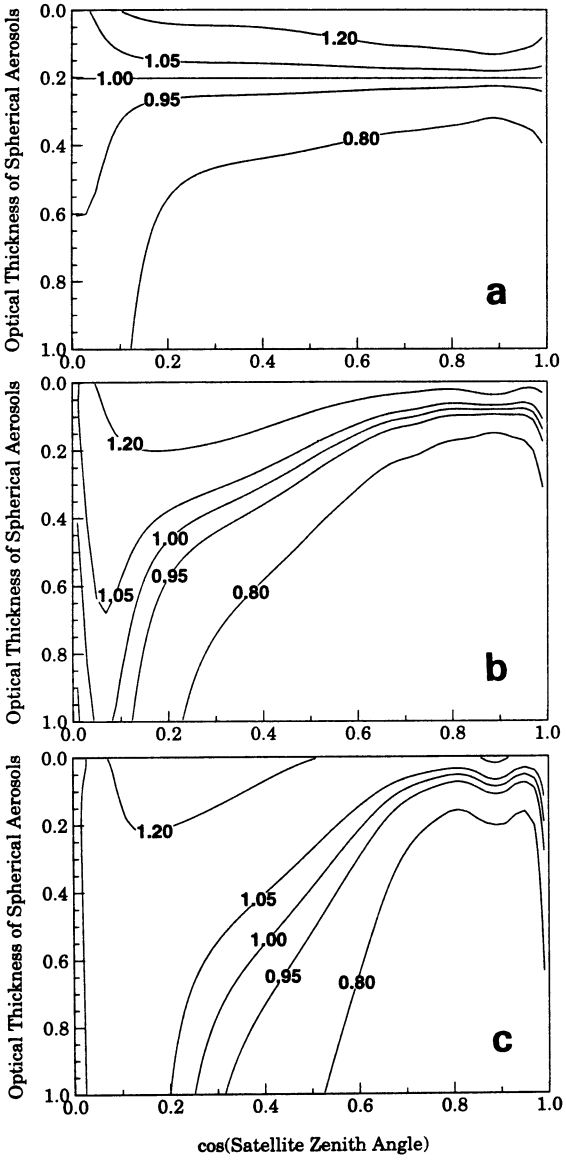

Figure 3. (a) Contour plot of the ratio of reflectivity computed for an atmosphere-ocean model containing spherical aerosols with optical thickness 0.2 and effective radius 1 μm relative to the reflectivity computed for the same model but with aerosol optical thickness τ_a continuously varying from 0 to 1. This ratio is plotted as a function of τ_a and cosine of satellite zenith angle. (b) As in (a), but for the ratio of reflectivity computed for nonspherical aerosols with optical thickness 0.2 relative to that for equivalent spherical aerosols with optical thickness varying from 0 to 1. (c) As in (b), but for r_{eff} = 2 μm.

Contours at levels not equal to 1 show the range of (erroneous) aerosol optical thickness that would be inferred if the aerosol size distribution, shape, and refractive index are still known *a priori*, but reflectivity measurements contain some error. We can conclude from Fig. 3a that the measurement accuracy for this idealized case must be better than ±5% if the accuracy of the aerosol optical thickness retrieval is to be better than ±20%.

By using the same approach we can illustrate the potential errors in the retrieved aerosol optical thickness that would result from the neglect of particle nonsphericity. Now, reflectances computed for a model atmosphere containing spheroidal aerosols with r_{eff} = 1 μm and a fixed optical thickness 0.2 are 'inverted' using the model of surface-equivalent spherical particles. Figure 3b is analogous to Fig. 3a but now shows a contour plot of the ratio ϱ of the reflectivity computed for the nonspherical aerosols with the optical thickness 0.2 relative to the reflectivity computed for equivalent spheres with optical thickness varying from 0 to 1. Again, the ϱ = 1 contour is the line plot of the retrieved optical thickness as a function of μ provided that the reflectance data are absolutely accurate, while the region between the contours at ϱ = 0.95 and 1.05 shows the range of uncertainty introduced by measurement errors not exceeding ±5%. It is quite evident that the retrieved optical thickness is strongly dependent on scattering geometry and can differ substantially from the actual value. Errors due to the neglect of particle nonsphericity are much larger than those due to measurement errors and can easily exceed 100%.

Comparison of Figs. 1 and 3b shows that the errors in the retrieved optical thickness follow the scattering angle dependence of the phase function ratio: the spherical model underestimates optical thickness at backscattering geometries (reflection toward the sun) and overestimates it at side-scattering geometries. As follows from Fig. 1, phase function differences increase with increasing effective radius, so we should expect even larger optical thickness errors for larger aerosol effective radii, as illustrated in Fig. 3c.

3. Effect of particle shape on the albedo of a cloud-free atmosphere

Asymmetry parameter of the phase function is calculated by integrating the phase function weighted by cosine of scattering angle over all scattering angles. This integration averages out contrasting nonspherical-spherical differences in phase function at various scattering angle ranges, making the resulting nonspherical asymmetry parameters very close to those for equivalent spheres (Fig. 2). Similarly, local albedo is obtained by integrating the reflection function weighted by μ over all angles of reflection. Therefore, despite large nonspherical-spherical differences in bidirectional reflectance (Figs. 3b and 3c), we may expect much smaller differences in local albedo. That this is indeed the case is demonstrated by Fig. 4 which shows the local albedo for a simple cloud-free model composed of an aerosol layer of optical thickness 0.2 above a Lambertian surface with albedo A_L. It is seen that local albedos computed for spheroidal and equivalent spherical aerosols with r_{eff} = 1.5 μm are in very good quantitative agreement, and further integration over all angles of illumination makes the corresponding global albedos (0.054 for spheroids and 0.052 for spheres if A_L = 0.02 and 0.530 for both spheroids and spheres if A_L = 0.6) essentially identical. Thus, for climate modeling applications, where only radiative flux and albedo information is required, Mie scattering calculations for equivalent spheres appear to give adequate

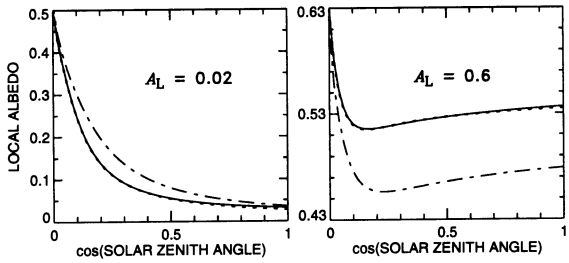

Figure 4. Local albedo vs cosine of solar zenith angle for nonspherical (solid lines) and equivalent spherical (dotted lines) aerosols with optical thickness 0.2 above a Lambertian surface with albedo A_L. The wavelength is 0.63 μm. Dot-dashed lines show plane albedo for spherical aerosols with optical thickness 0.4.

accuracy, even if real aerosols are nonspherical, as long as the aerosol optical depth and size distribution are accurately known.

4. Conclusions

Three important conclusions can be derived from our comparison of nonspherical and spherical cases.

(1) Even moderate nonsphericity of dust-like tropospheric aerosols can cause large errors in the retrieved aerosol optical thickness if satellite reflectance measurements over the ocean are analyzed using conventional Mie theory for spherical particles. The errors increase with increasing particle size and, depending on scattering geometry, can easily exceed 100%. These errors can be significantly larger than the minimum accuracy necessary for the long-term monitoring of global climate forcings and feedbacks [*DelGenio*, 1993].

(2) Instruments that provide near-simultaneous radiance measurements for a given scene at different viewing angles have a distinct advantage over radiometers scanning the earth in a plane perpendicular to the subsatellite path. Indeed, the very fact of viewing-angle dependence of the retrieved aerosol optical thickness can be evidence of particle nonsphericity (Fig. 3) and may be used to reject unreasonable aerosol models.

(3) If the aerosol optical thickness and size distribution are already known, e.g., retrieved from analyses or remotely sensed data or prescribed by a tracer model [*Tegen and Lacis*, 1995], then Mie theory can be used to compute the aerosol radiative forcing with adequate accuracy even if aerosols are nonspherical.

Importantly, conclusions 1 and 3 mean that no cancellation of errors occurs if one consistently uses Mie theory in the retrieval algorithm and then in computing the albedo for the retrieved aerosol optical thickness. This is demonstrated in Fig. 4 where dot-dashed lines show albedos computed for the same spherical particles but with 'erroneously retrieved' optical thickness 0.4.

Of course, particle nonsphericity is not the only factor that can result in errors in the retrieved aerosol optical thickness. Additional sources of errors are uncertainties in aerosol size distribution and refractive index which can contribute to uncertainties in aerosol phase function and single scattering albedo [*Wang and Gordon*, 1994]. Therefore, it will be important to analyze the combined effect of particle shape, size distribution, and refractive index on the accuracy of aerosol optical thickness, phase function, and single-scattering albedo retrievals, especially in those cases when reflectance measurements are available only at a limited range of scattering angles. It is interesting to note in this regard that, as our computations show, the errors in the retrieved aerosol optical thickness resulting from the use of Mie theory for nonspherical particles can be much larger that those resulting from an uncertainty in the aerosol real refractive index within ± 0.05 and an uncertainty in the imaginary refractive index within a factor of 2.

Acknowledgments. This work was supported in part by the NASA Office of Mission to Planet Earth and the Earth Observing System Project.

References

d'Almeida, G. A., P. Koepke, and E. P. Shettle, *Atmospheric Aerosols*, DEEPACK, Hampton, VA, 1991.

DelGenio, A., Accuracy requirements, in NASA Conf. Publ. 3234, 13-19, 1993.

Flatau, P., Ph.D. thesis, Colorado State University, Ft. Collins, CO, 1992.

Hansen, J.E., and A.A. Lacis, Sun and dust vs greenhouse gases: an assessment of their relative roles in global climate change, *Nature*, *346*, 713-719, 1990.

Hansen, J.E., and L.D. Travis, Light scattering in planetary atmospheres, *Space Sci. Rev.*, *16*, 527-610, 1974.

Hansen, J., W. Rossow, and I. Fung, eds., *Long-Term Monitoring of Global Climate Forcings and Feedbacks*, NASA Conf. Publ. 3234, 1993.

Hill, S.C., A.C. Hill, and P.W. Barber, Light scattering by size/shape distributions of soil particles and spheroids, *Appl. Opt.*, *23*, 1025-1031, 1984.

Koepke, P., and M. Hess, Scattering functions of tropospheric aerosols: the effect of nonspherical particles, *Appl. Opt.*, *27*, 2422-2430, 1988.

Kuik, F., P. Stammes, and J. W. Hovenier, Experimental determination of scattering matrices of water droplets and quartz particles, *Appl. Opt.*, *30*, 4872-4881, 1991.

Mishchenko, M. I., Light scattering by randomly oriented axially symmetric particles, *J. Opt. Soc. Am. A*, *8*, 871-882, 1991.

Mishchenko, M.I., and L.D. Travis, T-matrix computations of light scattering by large spheroidal particles, *Opt. Comm.*, *109*, 16-21, 1994a.

Mishchenko, M.I., and L.D. Travis, Light scattering by polydispersions of randomly oriented spheroids with sizes comparable to wavelengths of observation, *Appl. Opt.*, *33*, 7206-7225, 1994b.

Nakajima, T., M. Tanaka, M. Yamano, M. Shiobara, K. Arao, and Y. Nakanishi, Aerosol optical characteristics in the yellow sand events observed in May, 1982 at Nagasaki. 2. Models, *J. Meteorol. Soc. Japan*, *67*, 279-291, 1989.

Okada, K., A. Kobayashi, Y. Iwasaka, H. Naruse, T. Tanaka, and O. Nemoto, Features of individual Asian dust-storm particles collected at Nagoya, Japan, *J. Meteorol. Soc. Japan*, *65*, 515-521, 1987.

Penner, J.E., R.J. Charlson, J.M. Hales, N.S. Laulainen, R. Leifer, T. Novakov, J. Orgen, L.F. Radke, S.E.Schwartz, and L. Travis, Quantifying and minimizing uncertainty of climate forcing by anthropogenic aerosols, *BAMS*, *75*, 375-400, 1994.

Perry, R.J., A.J. Hunt, and D.R. Huffman, Experimental determinations of Mueller scattering matrices for nonspherical particles, *Appl. Opt.*, *17*, 2700-2710, 1978.

Rao, C.R., L.L. Stowe, and E.P. McClain, Remote sensing of aerosols over the oceans using AVHRR data. Theory, practice, and applications, *Int. J. Remote Sens.*, *10*, 743-749, 1989.

Tegen, I., and A. A. Lacis, Modeling of particle size distribution and its influence on the radiative properties of mineral dust aerosol, *J. Geophys. Res.*, submitted, 1995.

von Hoyningen-Huene, W., and M. Wendisch, Variability of aerosol optical parameters by advective processes, *Atmos. Environ.*, *28*, 923-933, 1994.

Wang, M., and H.R. Gordon, Estimating aerosol optical properties over the oceans with the multiangle imaging spectroradiometer: some preliminary results, *Appl. Opt.*, *33*, 4042-4057, 1994.

Waterman, P.C., Symmetry, unitarity, and geometry in electromagnetic scattering, *Phys. Rev. D*, *3*, 825-839, 1971.

M. I. Mishchenko, NASA GISS/SSAI, 2880 Broadway, New York, NY 10025 (crmim@nasagiss.giss.nasa.gov).

A. A. Lacis, B. E. Carlson, and L. D. Travis, NASA GISS, 2880 Broadway, New York, NY 10025.

(Received December 29, 1994; accepted February 22, 1995)